

Intermuscular tendons are essential for the development of vertebrate stomach

Ludovic Le Guen, Cécile Notarnicola and Pascal de Santa Barbara*

Gastrointestinal motility is ensured by the correct coordination of the enteric nervous system and the visceral smooth muscle cells (SMCs), and defective development of SMCs results in gut malformations and intestinal obstructions. In order to identify the molecular mechanisms that control the differentiation of the visceral mesenchyme into SMCs in the vertebrate stomach, we developed microarrays to analyze the gene expression profiles of undifferentiated and differentiated avian stomachs. We identify *Scleraxis*, a basic-helix-loop-helix transcription factor, as a new marker of stomach mesenchyme and find that expression of *Scleraxis* defines the presence of two tendons closely associated to the two visceral smooth muscles. Using targeted gene misexpression, we show that FGF signaling is sufficient to induce *Scleraxis* expression and to establish two tendon domains adjacent to the smooth muscle structures. We also demonstrate that the tendon organization is perturbed by altering *Scleraxis* expression or function. Moreover, using primary cells derived from stomach mesenchyme, we find that undifferentiated stomach mesenchyme can give rise to both SMCs and tendon cells. These data show that upon FGF activation, selected stomach mesenchymal cells are primed to express *Scleraxis* and to differentiate into tendon cells. Our findings identify a new anatomical and functional domain in the vertebrate stomach that we characterize as being two intermuscular tendons closely associated with the visceral SMC structures. We also demonstrate that the coordinated development of both tendon and smooth muscle domains is essential for the correct morphogenesis of the stomach.

KEY WORDS: FGF pathway, *Scleraxis*, Gut development, Tendon, Visceral smooth muscle, Chick

INTRODUCTION

The gastrointestinal (GI) tract is a remarkably complex, three-dimensional, specialized system derived from a simple tubular structure. The GI tract is composed of three germ layers: mesoderm (which forms the smooth muscle layer), endoderm (which forms the epithelial lining) and ectoderm [which includes the enteric nervous system (ENS)]. The primitive gut is initially a straight tube. As they develop, each region of the gut is characterized by a unique morphology discernible by gross and microscopic examination. These tissues show regional specific differentiation along the anteroposterior axis. This regionalization is maintained throughout life and is essential for the normal function of the adult gut. Candidate factors involved in gut development include genes that were first identified in *Drosophila*. These comprise homeotic (Hox and Nkx) and secreted factors [bone morphogenetic protein (BMP) and *Hedgehog*] (de Santa Barbara et al., 2002).

The motility of the GI tract is ensured by the correct coordination of the visceral smooth muscle cells (SMC) and the autonomous ENS. The ENS originates from neural crest cells that migrate from the dorsal region of the neural tube and colonize the whole gut to establish its innervation (Wallace and Burns, 2005). SMCs derive from the splanchnopleural mesoderm that will form the undifferentiated visceral mesenchyme (Roberts, 2000). Few have investigated the molecular mechanisms involved in the differentiation of the visceral mesenchyme into SMCs. SMCs are present in both vascular and digestive systems; however, the digestive tract is the most abundant contributor of SMCs in humans (Gabella, 2002). In the chick, the gizzard (muscular stomach or antrum) has a thick layer of smooth muscle that facilitates mechanical digestion, whereas the

proventriculus (glandular stomach or fundus), which develops anteriorly to the gizzard, has only a very thin smooth muscle layer (Roberts, 2000). The intestines show modest development of smooth muscle layers. In the avian stomach, SMC differentiation is observed from embryonic day (E) 9. Thus, the chick stomach offers an ideal model in which to elucidate the molecular mechanisms that control visceral SMC differentiation. In the GI tract, *Bmp4*, a ligand that belongs to the transforming growth factor β (TGF β) superfamily, is expressed in the mesenchyme of the whole chick gut with the exception of the gizzard (Roberts et al., 1998). When overexpressed, *Bmp4* causes a reduction in the thickness of the smooth muscle layer of the stomach, demonstrating a regulatory role in gut muscle growth (Roberts et al., 1998). Conversely, the homeotic gene *Bapx1* is expressed only in the chick gizzard mesenchyme and acts as a repressor of *Bmp4*, therefore modulating gizzard smooth muscle development (Nielsen et al., 2001). In addition, we have investigated the function of the BMP pathway during visceral SMC differentiation and found that aberrant modulation of BMP activity altered this process (de Santa Barbara et al., 2005).

In order to identify factors that trigger and control the differentiation of visceral SMC, we carried out a microarray screen to isolate candidate genes. We identified *Scleraxis*, a member of the basic-helix-loop-helix (bHLH) family of transcription factors, which is expressed in tendon cells of the stomach adjacent to the visceral SMC. We then used the avian retroviral system to specifically misexpress or inactivate *Scleraxis* in the stomach mesenchyme, and showed that *Scleraxis* expression defines the intermuscular tendon domains that are established in close association with the visceral SMC.

MATERIALS AND METHODS

Chick embryonic gastrointestinal tissues

Fertilized White Leghorn eggs were obtained from Haas Farm, France. Tissues were staged according to Hamburger and Hamilton for early embryogenesis stages and by embryonic day (E) for gastrointestinal tract analysis (Hamburger and Hamilton, 1951).

INSERM ERI 25, Muscle and Pathologies, 34295 Montpellier Cedex 05, France and University Montpellier I, EA4202, 34295 Montpellier Cedex 05, France.

*Author for correspondence (e-mail: Pascal.de-Santa-Barbara@inserm.fr)

Retroviral misexpression studies

The *Fgf8* (Brent and Tabin, 2004), sFgfR2b (Mandler and Neubuser, 2004) and GFP (Moniot et al., 2004) viral constructs have been previously described. Sh*Scleraxis* associated with the mouse U6 promoter and full-length avian *Scleraxis* cDNA were cloned into the shuttle vector Slax and then subcloned into the RCAS(A) vector. Full-length avian *Scleraxis* cDNA was cloned in frame in the Slax-Engrailed vector and then subcloned into the RCAS(A) vector. All vectors were transfected into avian DF-1 cell lines, and viruses harvested and titered using standard techniques. To target the presumptive stomach mesenchyme, misexpression experiments were performed on stage 9-10 embryos, as previously described (Moniot et al., 2004).

Primary cell cultures derived from stomach mesenchyme

Gizzards from stage 25 (referred to as E5 gizzards) were harvested in PBS solution. After collagenase treatment (Sigma) at room temperature for 12 minutes, we isolated the mesenchymal layer using fine forceps (Simon-Assman and Kédinger, 2000). Individual mesenchymal cells were plated on dishes and kept in culture for 24 (E5+1D) and 72 hours (E5+3D) in DMEM, 10% fetal bovine serum in the absence or presence of the different avian retroviruses.

Expression analyses

In situ hybridization experiments on whole tissues/embryos and paraffin sections were carried out as previously described (Moniot et al., 2004). Different chick templates for antisense riboprobes were obtained by PCR amplification using specific primer sets (details of primers are available on request). The following plasmids were used: α *SMA*, *Type I Collagen*, *Fgf7*, *Fgf10*, *Fgfr1* (Edom-Vovard et al., 2001), *Fgfr2* (Brent and Tabin, 2004), *Fjx* (Yamaguchi et al., 2006), *Scleraxis* (gift from D. Duprez), *Sox10* (Moniot et al., 2004) and *Tenomodulin*. Immunohistochemistry was performed on paraffin sections using polyclonal antibodies against α *SMA* (Sigma) and Phospho-Histone H3 Ser10 (Upstate), and monoclonal antibodies against Type I Collagen, GAG and Decorin [Developmental Studies Hybridoma Bank (DSHB)].

In cellulo in situ hybridization was performed as previously described (Gregoire et al., 2006). Methyl violet staining was used as described (Bi et al., 2007). Immunofluorescence was performed using monoclonal antibodies directed against Tenascin (DSHB) and Type I Collagen (DSHB), and polyclonal antibodies against Caldesmon (Sigma), Desmin (Sigma) and Sox9 (Moniot et al., 2004). The Alexa 488 anti-mouse and Alexa 555 anti-rabbit secondary antibodies (Invitrogen) were used, and nuclei were stained with DAPI (Molecular Probes). Cells were mounted in FluorSave reagent (Calbiochem).

For microarray experiments and quantitative RT-PCR amplification, RNAs were extracted with the RNeasy Kit (Qiagen). Biotinylated complementary RNAs were hybridized to the Affymetrix GeneChip Chicken Genome Arrays using standard manufacturer's protocols (Affymetrix, IRB, CHU Montpellier, France). Fluorescence intensities were quantified and analyzed using the GCOS software (Affymetrix; see Table S1 in the supplementary material). *Scleraxis* expression was quantified by quantitative RT-PCR amplification using LightCycler technology (Roche Diagnostics; 95°C for 10 seconds, 60°C for 5 seconds, 72°C for 10 seconds). PCR primers are available on request. mRNA values were determined by LightCycler analysis software (version 3.1), according to the standard curves. Data were represented as the relative mean level of *Scleraxis* expression relative to *18S* standard expression.

For electron microscopy, tissues were immersed in a solution of 3.5% glutaraldehyde in phosphate buffer (0.1 M, pH 7.4) overnight at 4°C. They were then washed and post-fixed in 1% osmic acid plus 0.8% potassium ferrocyanide in the dark at room temperature for 2 hours. After washing, tissues were dehydrated in graded ethanol solutions and embedded in EmBed 812 DER 736. Thin sections (85 nm; Leica-Reichert Ultracut E) were collected. Sections were counterstained with uranyl acetate and lead citrate, and observed using a Hitachi 7100 transmission electron microscope at the CRIC facility (C. Cazevielle, Montpellier, France).

Photography

Images of whole-mount tissues and paraffin sections were collected with a Nikon DXM1200 camera connected to a Nikon Multizoom AZ100 microscope.

RESULTS

Intermuscular tendons are present in the vertebrate stomach

In order to identify factors that play a role at the onset of differentiation of the visceral SMC, we used microarrays to compare the gene expression profiles of undifferentiated E6 and differentiated E9 chick gizzards (Fig. 1A; see also Table S1 in the supplementary material). We observed a higher expression of well-known smooth muscle markers, such as *Caldesmon*, *Desmin*, *Smooth Muscle Myosin*, *Smooth Muscle Actin*, and of more recently discovered ones, such as *Smoothelin* and *SRF* in E9 gizzards (Wallace and Burns, 2005; Niessen et al., 2005; Mericskay et al., 2007). We also identified a new cluster composed of genes (i.e. *Scleraxis*, *Decorin*, *Tenomodulin* and *Type XII Collagen*) that are associated with the development and differentiation of tendon tissues (Tozer and Duprez, 2005).

In this study, we focused on *Scleraxis*, a member of the bHLH family of transcription factors previously reported as an early marker of tendons and tenocytes (Edom-Vovard et al., 2001; Schweitzer et al., 2001). We next examined the expression profile of *Scleraxis* during GI tract development and found it expressed in two specific subdomains of the stomach mesenchyme from E6 to E9, and at the boundaries of these two domains after SMC differentiation (E12; Fig. 1B). At E9, *Scleraxis* was expressed also in the caecum, a structure that separates the colon from the small intestine (see Fig. S1 in the supplementary material).

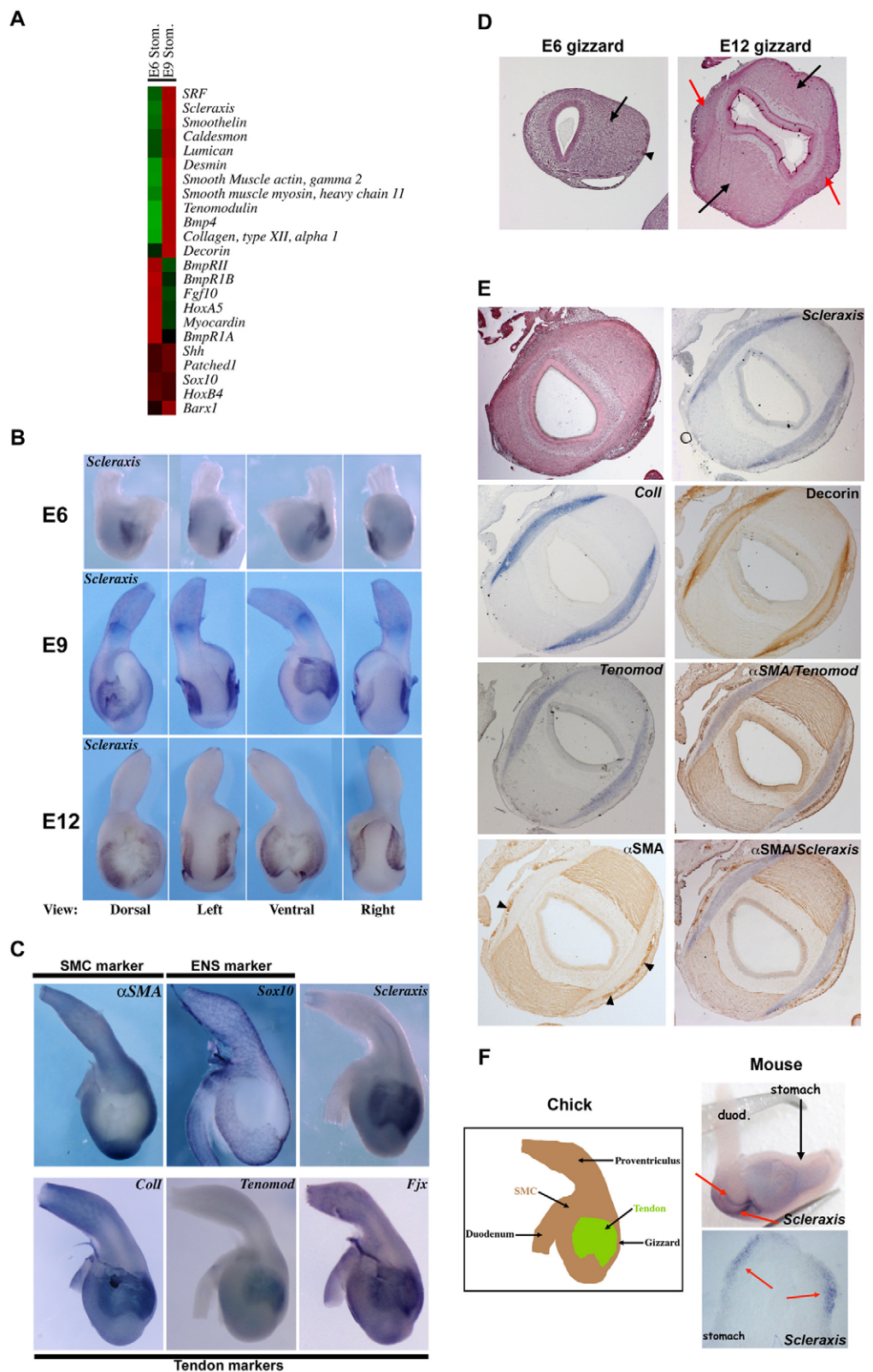
The mesenchyme of the avian embryonic stomach is composed of visceral SMC (that expresses α *SMA*, a SMC-specific factor) and intercalated ENS cells (positive for *Sox10*) to allow autonomous contraction. However, the expression of *Scleraxis* and α *SMA* or *Sox10* was mutually exclusive (Fig. 1C), suggesting that *Scleraxis* is expressed neither in visceral SMC nor in ENS cells. Analyses by light microscopy of the embryonic gizzard showed a homogenous visceral mesenchymal structure with migrating ENS cells in the outer layer at E6 (Fig. 1D). Conversely, at E12, the gizzard consisted of two well-differentiated smooth muscle areas both associated with two connective structures (Fig. 1D), which, at E9, appeared to be close to the differentiating SMC (Fig. 1E). These connective tissues were positive for *Scleraxis*, *Tenomodulin* (another gene identified by our microarray screen) and other tendon markers, such as *Type I Collagen* (Ros et al., 1995), *Four-jointed* (Yamaguchi et al., 2006) and *Decorin*, all of which showed an expression pattern overlapping with that of *Scleraxis* (Fig. 1C,E) in these two connective tissues. Conversely, *Scleraxis* and α *SMA* were detected in two specific and mutually exclusive domains (Fig. 1E). Furthermore, we found that, in the mouse, *Scleraxis* expression was limited to two small domains in the antrum that correspond to the avian gizzard (Fig. 1F).

An early study highlighted the intimate relation between muscle bundles and these two connective structures in the adult avian gizzard (Watzka, 1932); two centra tendinea were observed in the adult gizzard and were characterized as being rich in collagen fibrils (McLelland, 1979; Gabella, 1985). Attachment of two skeletal muscles through a central structure was also described in the diaphragm. This was considered to be another category of tendon and was named an intermuscular tendon

Fig. 1. Intermuscular tendons are present in the embryonic stomach.

(A) Relative expression level of transcripts in E6 and E9 chick gizzards; the highest signals are in red, lowest in green. At E9, smooth muscle and tendon markers are expressed at higher levels than at E6. **(B)** Expression pattern of *Scleraxis* in the stomach by whole-mount in situ hybridization using an antisense *Scleraxis* riboprobe. *Scleraxis* expression is restricted to two newly identified domains located on the dorsal and ventral sides of the gizzard. From E6 to E9, the *Scleraxis* expression domain widens. At E12, *Scleraxis* expression is restricted to the boundaries of these initial domains. **(C)** Whole-mount in situ hybridization on E9 stomachs. α SMA is expressed in SMC and *Sox10* in ENS cells. *Scleraxis*, *Type I Collagen* (*Coll*), *Tenomodulin* and *Four jointed* (*Fjx*) are expressed mainly in the tendon domains. All tendon markers show a pattern of expression that overlaps with that of *Scleraxis*, whereas they are absent from the smooth muscle domains and ENS cells. **(D)** Histology of E6 and E12 gizzards. At E6 the visceral mesenchyme is homogenous (arrow), in spite of the presence of migrating enteric nervous cells on the outer layer (arrowhead). At E12, the gizzard is composed of two well-differentiated smooth muscle structures (black arrows) adjacent to two domains composed of connective tissue (red arrows).

(E) Serial transversal sections of an E9 gizzard. *Scleraxis*, *Tenomodulin* and *Type I Collagen* are detected by in situ hybridization, and α SMA and Decorin by immunostaining. Two differentiated smooth muscle structures are associated with the two emerging domains of connective tissues characterized by the specific expression of *Scleraxis* and of the tendon cell markers *Type I Collagen*, *Decorin* and *Tenomodulin*. α SMA labels the two smooth muscle areas as well as the monolayer of smooth muscle tissue surrounding the vasculature (arrowheads). In situ hybridization of *Scleraxis* or *Tenomodulin* followed by α SMA immunodetection on the same sections demonstrated the presence of two tendon structures closely associated with the visceral smooth muscle structures of the gizzard. **(F)** Left panel: schematic representation of avian E9 stomach indicating the presence of intermuscular tendons, the visceral SMC domain (brown area), and the well-organized tendon domain (green area). Right panels: in situ hybridization on mouse E13 stomachs using a mouse *Scleraxis* antisense riboprobe (whole-mount and section). Two *Scleraxis* expression domains (red arrows) are visible.



(Ackerman and Greer, 2007; Murchison et al., 2007). Taken together, these data indicate that, in the stomach, *Scleraxis* exhibits a restricted expression pattern that defines two tendons closely associated to the two visceral smooth muscles (Fig. 1F). We define them as intermuscular tendons.

FGF signaling pathway is necessary and sufficient to establish the tendon domains

Previous studies have shown that the fibroblast growth factor (FGF) signaling pathway is required for the induction of *Scleraxis* expression in somitic tendon progenitors and for its maintenance in chick limb tendons (Brent and Tabin, 2004; Edom-Vovard et al., 2002). In order to identify the FGF ligand(s) and receptor(s) that could be responsible for the initiation of *Scleraxis* expression in E6 stomach, we quantified by RT-PCR their levels in E6 gizzards, and detected robust expression of eight FGF ligands and three FGF receptors (Fig. 2A). Whole-mount in situ hybridization revealed that *Fgf7*, *Fgf10*, *Fgfr1* and *Fgfr2* were expressed in the gizzard mesenchyme from E6 (Fig. 2B; see also Fig. S2 in the supplementary material). The other detected FGF ligands were expressed mainly in the epithelial layer (our unpublished data). We then investigated whether the FGF signaling pathway could regulate *Scleraxis* expression. With this aim, we perturbed the FGF pathway by misexpressing an inhibitory form of the mouse FGFR2 IIb receptor (referred to as sFgfr2b) that is secreted and preferentially sequesters the FGF ligands 1, 3, 7 and 10 (Mandler and Neubuser, 2004), and then monitored *Scleraxis* expression by in situ hybridization and quantitative RT-PCR (Fig. 2C,D). In the gizzard, infection with RCAS-sFgfr2b retroviruses led to a downregulation of *Scleraxis* expression and a size reduction of the two specific domains (Fig. 2C), whereas expression of RCAS-GFP, a negative control, had no effect on *Scleraxis* (compare Fig. 2C with Fig. 1B). Efficient retroviral infection of the mesenchyme was confirmed by immunohistochemistry using antibodies against the avian retroviral GAG protein (α 3C2), or by in situ hybridization using a riboprobe against the avian retroviral *env* gene (*env*; data not shown). We monitored the *Scleraxis* mRNA level by quantitative RT-PCR and observed a strong decrease in RCAS-sFgfr2b in the stomach; this finding was supported also by the observed reduction of *Fgf10* mRNA in this condition (Fig. 2D). Conversely, ectopic activation of the FGF signaling pathway along the GI tract following RCAS-*Fgf8* misexpression caused multiple morphological defects, mainly in the proventriculus, the gizzard and the caecum (Fig. 2E; see also Fig. S3 in the supplementary material). RCAS-*Fgf8*-infected stomachs showed ectopic expression of *Scleraxis* associated with other tendon markers, such as *Type I Collagen* and *Tenomodulin* (Fig. 2E; Figs S4 and S5 in the supplementary material). Moreover, in RCAS-*Fgf8*-infected stomachs, we observed reduced expression of α SMA in the areas of ectopic expression of the tendon markers (Fig. 2E; Fig. S3 in the supplementary material). To analyze the effect of FGF activation on cell proliferation, we used antibodies directed against phosphorylated Histone 3B (PH3), a standard cell cycle marker of the G2/M transition (Fig. 2F). We did not observe significant differences in the number of proliferative cells in the gizzard SMCs following infection of RCAS-*Fgf8* or RCAS-GFP, indicating that FGF activation does not induce a global upregulation of the mitotic potential. These data suggest that the FGF signaling pathway controls positively the establishment of tendons in the developing stomach, and recruits mesenchymal cells towards a tendon fate.

Tendon structures are essential for the development of the stomach

Scleraxis belongs to the bHLH family of transcription factors and is one of the rare transcription factors expressed at the onset of tendon development (Edom-Vovard et al., 2001; Schweitzer et al., 2001). In order to investigate more directly the role of *Scleraxis* in stomach development, we used a loss-of-function technique that involved delivering Sh*Scleraxis* to the chick stomach in vivo (Fig. 3A,B) (Harpavat and Cepko, 2006). First, we tested the efficiency of RCAS-Sh*Scleraxis* in primary cells derived from stomach mesenchyme and observed a robust reduction of *Scleraxis* mRNA (Fig. 3C) without any side effect on the identity of the infected cells (data not shown). In embryonic stomachs, RCAS-Sh*Scleraxis* led to a strong downregulation of *Scleraxis* expression (Fig. 3D) and to some minor defects, such as a smaller gizzard and a straight proventriculus (Fig. 3D). Strong retroviral infection was correlated with decreased expression of *Scleraxis*, *Type I Collagen* and *Tenomodulin* (Fig. 3E), suggesting a reduction in size of the tendon domains in the developing stomach. Conversely, we observed an increase of the territory labeled by α SMA, a SMC marker (Fig. 3E).

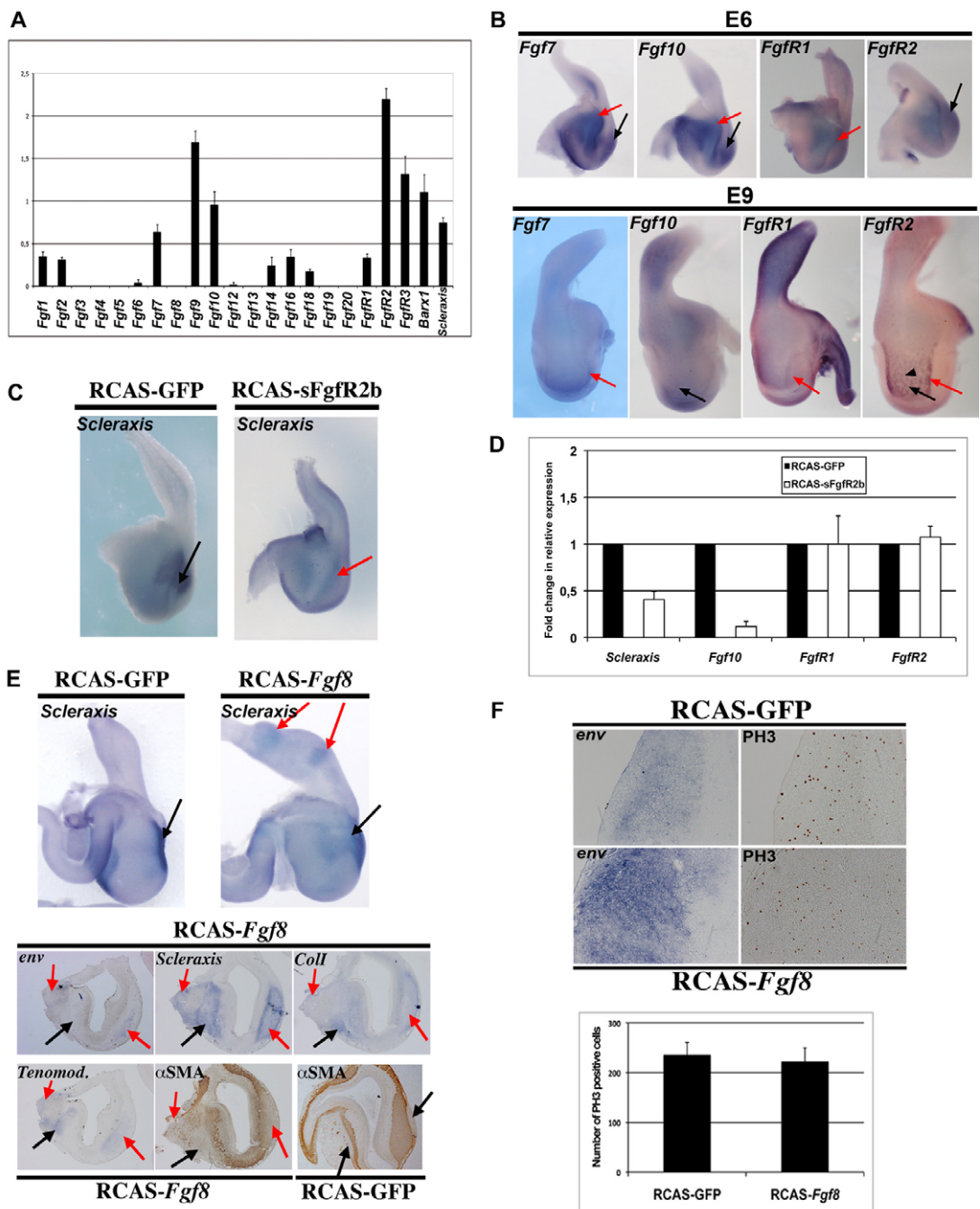
We next used a gain-of-function approach and ectopically misexpressed full-length *Scleraxis* along the GI tract (Fig. 4). Although we misexpressed *Scleraxis* in different regions of the digestive system, we observed effects only in the stomach (Fig. 4). *Scleraxis* misexpression induced a gross phenotype characterized by an aberrantly dilated gizzard associated with a curved proventriculus (Fig. 4A). RCAS-*Scleraxis* expressing cells were highly concentrated and organized around territories of endogenous expression (Fig. 4A), whereas the muscle domains were strongly reduced, as revealed by an α SMA riboprobe (Fig. 4A). Although RCAS-*Scleraxis* expression was correlated with α SMA inhibition, we did not observe an ectopic induction of *Type I Collagen*, as we had in the case of RCAS-*Fgf8* misexpression (compare Fig. 4B with Fig. 2E).

Scleraxis is considered to be a gene activator and recently *Type I Collagen* has been identified as a target in tendon fibroblasts (Lejard et al., 2007). Therefore, we thought that by converting *Scleraxis* into a transcriptional repressor, we could block the expression of target genes and counteract its activator function. With this aim, we fused the Engrailed repressor domain in frame to *Scleraxis* and misexpressed RCAS-*Scleraxis*-Engrailed in the stomach to repress endogenous *Scleraxis* function. In embryonic stomachs, RCAS-*Scleraxis*-Engrailed led to some minor defects, comparable to those observed in RCAS-Sh*Scleraxis* stomachs (data not shown). *Type I Collagen* expression was strongly inhibited in the infected tendon domain and this inhibition was associated with defects in the tendon structure (Fig. 4C). Recently, others genes known to be expressed specifically in the tendons, such as *Tenomodulin* and *Type XIV Collagen*, were demonstrated to be targeted by *Scleraxis* in the limb (Shukunami et al., 2006; Murchison et al., 2007). In contrast to the limb tendon, we found that *Type XIV Collagen* was not expressed in the intermuscular tendon but only in gastric ENS cells (see Fig. S6 in the supplementary material). Using quantitative RT-PCR to analyze the expression levels of *Tenomodulin*, we observed that *Scleraxis* misexpression in the gizzard upregulated *Tenomodulin*, whereas ectopic expression of *Scleraxis* in the proventriculus did not (Fig. 4D). Moreover, *Scleraxis*-Engrailed expression in the gizzard strongly repressed *Tenomodulin* expression (Fig. 4D). These findings demonstrate that, during the development of the intermuscular tendon, *Scleraxis* is upstream of *Type I Collagen* and *Tenomodulin*, and strongly suggest that *Type I Collagen* and *Tenomodulin* are in vivo targets of *Scleraxis* in the stomach.

Fig. 2. The FGF signaling pathway is necessary and sufficient to establish the stomach tendon structures.

(A) Semi-quantitative RT-PCR analysis of FGF ligand and receptor expression in E6 gizzards. Shown are the mean values \pm s.e.m. relative to the 18S ribosomal RNA control. Each measurement was done on four independent cDNA preparations ($n=4$).

(B) Whole-mount in situ hybridization on E6 and E9 stomachs. At E6, *Fgf7*, *Fgf10*, *Fgfr1* and *Fgfr2* are widely expressed in the gizzard mesenchyme. At E9, *Fgf7* and *Fgfr1* expression becomes restricted to the mesenchyme close to the edge of the tendon domains, and *Fgf10* and *Fgfr2* are both expressed in ENS cells; in addition, *Fgfr2* expression defines the tendon borders. Red arrows indicate the tendon area, black arrows the mesenchyme or smooth muscle domain, arrowhead the ENS cells. (C) Inhibition of the FGF signaling pathway in the stomach affects *Scleraxis* expression. Whole-mount in situ hybridization with an antisense *Scleraxis* riboprobe on E9 stomachs in which GFP (RCAS-GFP) and sFgfR2b (RCAS-sFgfR2b) are misexpressed. GFP misexpression does not alter stomach morphology, while sFgfR2b misexpression affects slightly the size of the gizzard. The *Scleraxis* expression domain is downregulated in sFgfR2b-misexpressing stomachs (red arrow), although it is not affected in GFP-misexpressing stomachs (black arrow). (D) Inhibition of the FGF signaling pathway in the stomach affects *Scleraxis* and *Fgf10* but not *Fgfr1* and *Fgfr2* expression. Quantitative RT-PCR experiments on E7 stomachs in which RCAS-GFP (control) and RCAS-sFgfR2b were misexpressed. sFgfR2b infected stomachs express 60% less *Scleraxis* and 90% less *Fgf10* than do controls. Each measurement was done on two independent cDNA preparations ($n=4$). (E) Activation of the FGF signaling pathway in the stomach affects the expression of *Scleraxis* and specific tendon markers. Whole-mount in situ hybridization using an antisense *Scleraxis* riboprobe on RCAS-GFP and RCAS-*Fgf8* E9 stomachs. Ectopic activation of the FGF pathway through *Fgf8* misexpression induces ectopic mesenchymal buddings associated with ectopic expression of *Scleraxis* in the proventriculus (red arrows). Serial adjacent longitudinal sections of a RCAS-*Fgf8* E9 stomach analyzed by in situ hybridization with specific antisense riboprobes directed against *Env*, *Scleraxis*, *Tenomodulin* and *Type I Collagen*, and by immunohistochemistry with an anti- α SMA antibody. Longitudinal section of a RCAS-GFP E9 stomach analyzed by immunohistochemistry with an anti- α SMA antibody. Areas with RCAS-*Fgf8*-expressing cells, detected by *Env*, are characterized by the presence of *Scleraxis* and other tendon markers, such as *Tenomodulin* and *Type I Collagen*, and by reduction of the α SMA-positive domain. Black arrows indicate endogenous tendon structures; red arrows, ectopic tendons. (F) Serial longitudinal sections of E9 stomach infected with RCAS-*Fgf8* and RCAS-GFP retroviruses and analyzed by in situ hybridization with an *Env* riboprobe and by immunohistochemistry with an anti-PH3 antibody. Positive signals were counted in three comparable sections. Misexpression of *Fgf8* in the gizzard had no effect on proliferation.



However, *Scleraxis* alone cannot induce ectopic expression of *Type I Collagen*, suggesting the necessity of an additional interacting partner(s).

We then analyzed by electron microscopy the ultrastructure of visceral SMC after infection with different retroviral constructs (Fig. 5). In control gizzards (Fig. 5A), tendon cells showed predominantly rough endoplasmic reticulum and mitochondria, and were surrounded by collagen fibrils; visceral SMC, by contrast, presented mainly intracellular actin formation and thick cytoplasm. In addition, tendon cells were elongated, whereas SMC were rounded. In RCAS-*Fgf8* gizzards, SMC were elongated with numerous filopodia and no intracellular actin formation, but numerous organelles and ectopic collagen fibrils were observed in the intercellular region. These ectopic fibrils were not observed in RCAS-*Scleraxis* SMC. However, ectopic expression of *Scleraxis* in the gizzard SMC inhibited the formation of intracellular actin and was associated with the presence of numerous organelles (Fig. 5A). Tendon cells, in which sFgFR2b, *ShScleraxis* and *Scleraxis*-*Engrailed* were misexpressed, showed an absence or a strong reduction of collagen fibrils in the intercellular region (Fig. 5B). Moreover, in

each of the three conditions ectopic cells with thick cytoplasm, which are not observed in normal tendon cells, were present (compare Fig. 5B with 5A).

In summary, our data indicate that tendon structures are important for the regulated development of the stomach, and that their differentiation is closely coordinated with that of visceral smooth muscles.

Undifferentiated stomach mesenchymal cells give both SMCs and tendon cells

We showed that tendon and smooth muscle domains are closely associated in the stomach and that activation of the FGF pathway in the anterior and posterior parts of the stomach mesenchyme induces ectopic tendon domains (Fig. 2), suggesting that modulation of this pathway in the visceral mesenchyme is sufficient to pattern the tendon. To evaluate the capacity of undifferentiated visceral mesenchyme to give rise to tendon cells, we set up primary cell cultures derived from stage 25 gizzards before the onset of *Scleraxis* expression in the stomach. Throughout the study, we refer to stage 25 gizzard mesenchyme as E5 gizzard mesenchyme. With this aim, we adapted a reliable

Fig. 3. Inhibition of *Scleraxis* expression in the stomach impairs its normal development.

(A) Sequence of the sense oligonucleotide (21 red nucleotides) from the avian *Scleraxis*-coding sequence that makes the hairpin and specifically inhibits its expression.

(B) To deliver *ShScleraxis* into the chick stomach in vivo, the hairpin, the expression of which was under the control of the mouse U6 promoter, was cloned into the RCAS viral vector.

(C) Real-Time RT-PCR amplification of dissected E5 gizzard mesenchymal-derived cells cultured for 3 days after infection with RCAS-*ShScleraxis*. Infected cells express 85% less *Scleraxis* transcripts than do control cells (RCAS-GFP). Each measurement was done on two independent cDNA preparations ($n=4$).

(D) Inhibition of *Scleraxis* expression in RCAS-*ShScleraxis* stomachs. Whole-mount in situ hybridization using the antisense *Scleraxis* riboprobe on E6 stomachs in which RCAS-GFP and RCAS-*ShScleraxis* are misexpressed.

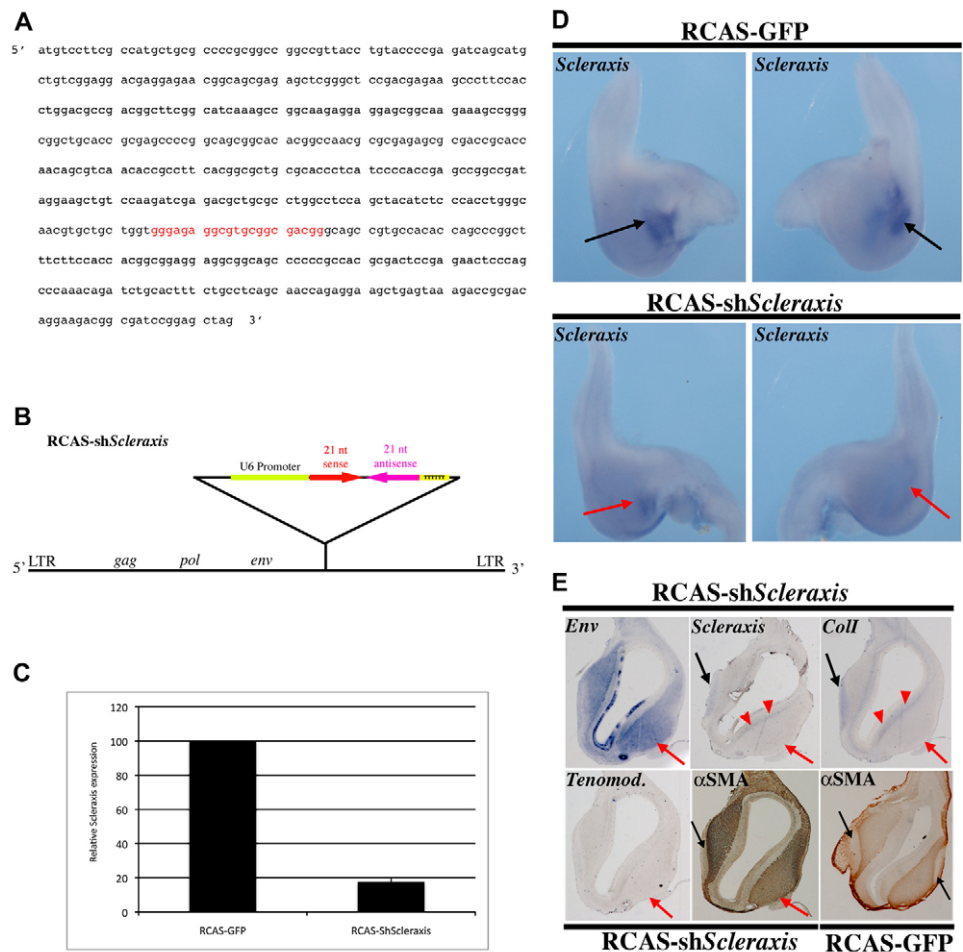
RCAS-*ShScleraxis* stomachs present a slight defect characterized by thinner gizzard and straight proventriculus compared with RCAS-GFP controls.

These defects are associated with a diminution of *Scleraxis* expression. Black arrows indicate normal *Scleraxis* expression in the tendon structures and red arrows show the decrease of *Scleraxis* expression in the tendon domains.

(E) Serial longitudinal sections of an E9 RCAS-*ShScleraxis* stomach analyzed by in situ hybridization with specific antisense riboprobes directed against *Env*, *Scleraxis*, *Type I Collagen* and *Tenomodulin*, and by immunohistochemistry with an anti- α SMA antibody.

Longitudinal section of a RCAS-GFP E9 stomach analyzed by immunohistochemistry with an anti- α SMA antibody. Areas with RCAS-*ShScleraxis*-expressing cells, detected with the *Env* probe, are characterized by a strong decrease in the expression of *Scleraxis*, *Type I Collagen* and *Tenomodulin*, and an increase of the α SMA-positive domain.

Note the aberrant localization of a few *Scleraxis*- and *Type I Collagen*-expressing cells in the submucosal layer close to the gastric epithelium (red arrowheads). Black arrows indicate endogenous tendon structures; red arrows, areas where RCAS-*ShScleraxis* is strongly expressed.



(E) Serial longitudinal sections of an E9 RCAS-*ShScleraxis* stomach analyzed by in situ hybridization with specific antisense riboprobes directed against *Env*, *Scleraxis*, *Type I Collagen* and *Tenomodulin*, and by immunohistochemistry with an anti- α SMA antibody. Longitudinal section of a RCAS-GFP E9 stomach analyzed by immunohistochemistry with an anti- α SMA antibody. Areas with RCAS-*ShScleraxis*-expressing cells, detected with the *Env* probe, are characterized by a strong decrease in the expression of *Scleraxis*, *Type I Collagen* and *Tenomodulin*, and an increase of the α SMA-positive domain. Note the aberrant localization of a few *Scleraxis*- and *Type I Collagen*-expressing cells in the submucosal layer close to the gastric epithelium (red arrowheads). Black arrows indicate endogenous tendon structures; red arrows, areas where RCAS-*ShScleraxis* is strongly expressed.

technique that allowed us to enzymatically separate the gizzard mesenchyme from its endodermal counterpart (Fig. 6A) (Simon-Assman and Kédinger, 2000). Next, E5 mesenchymal cells were cultured for one (E5+1D) and three days (E5+3D). At E5+1D, we observed that some isolated, scattered cells were positive for *Scleraxis* expression; at E5+3D, we observed the presence of several colonies that were all positive for *Scleraxis* expression (Fig. 6B). All *Scleraxis*-positive colonies were also visualized by staining with Methyl Violet, a specific histological tendon dye (Fig. 6C) (Bi et al., 2007). We then analyzed these colonies and found that they strongly expressed Type I collagen and Tenascin (tendon markers) (Tozer and Duprez, 2005), faintly expressed Desmin (mesenchymal derived cell marker) but did not express Caldesmon (SMC marker) or Sox9 (chondrocyte marker) (Lefebvre et al., 1997) (Fig. 6D). Conversely, we observed robust expression of Caldesmon and Desmin in the cells adjacent to the colonies, suggesting that visceral SMC organized around these structures (Fig. 6D).

We have shown that modulation of the FGF pathway and deregulation of *Scleraxis* expression are associated with reciprocal changes in visceral SMC and tendon cells of the stomach. We therefore assessed the colony-forming efficiency of E5 gizzard mesenchymal primary cultures in which we deregulated *Scleraxis* expression or the FGF pathway. The colony-forming efficiency was evaluated by Methyl Violet staining (Fig. 6E). We observed that RCAS-*Scleraxis* and particularly RCAS-*Fgf8* misexpression increased the number of colonies (Fig. 6E). RCAS-Sh*Scleraxis* did not affect the number of colonies, whereas RCAS-*Scleraxis*-*Engrailed* strongly inhibited their formation. However, RCAS-Sh*Scleraxis* colonies were smaller, with few cells compared with the control colonies (data not shown). We also analyzed the proliferation rate in these different cultures by immunohistochemistry using anti-PH3 antibodies (data not shown) and by quantitative RT-PCR to evaluate the level of *Pcna* RNAs (Fig. 6F) and did not observe, like in vivo, strong changes that could be responsible for the differences in colony formation.

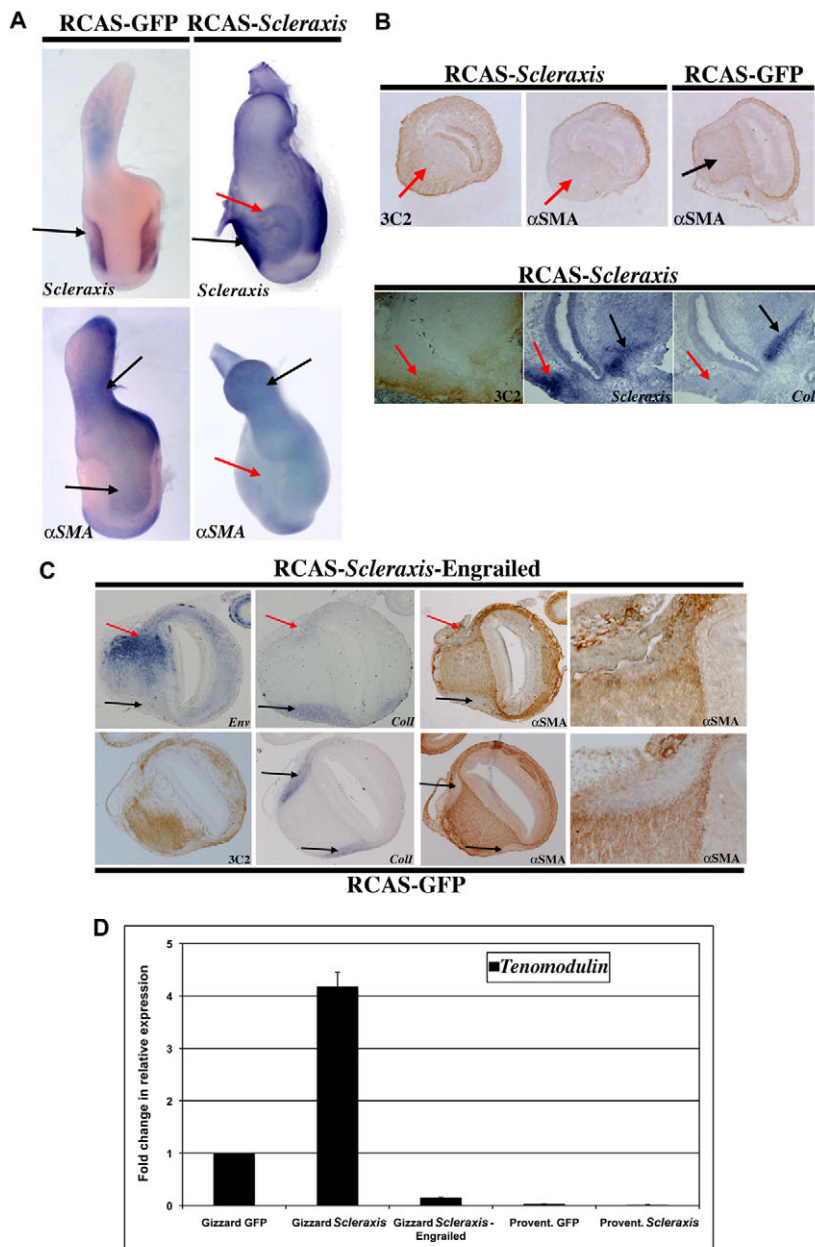


Fig. 4. Misexpression of *Scleraxis* in the whole stomach inhibits SMC differentiation. (A) Whole-mount in situ hybridization using the *Scleraxis* and α SMA riboprobes on E9 stomachs misexpressing GFP or *Scleraxis*. Ectopic *Scleraxis* expression (RCAS-*Scleraxis*) induces a gross phenotype characterized by dilated gizzard associated with a curved proventriculus, compared with RCAS-GFP controls. Furthermore, RCAS-*Scleraxis* inhibits the expression of the SMC marker α SMA. Upper black arrows indicate endogenous tendon structures; lower black arrows indicate normal SMC domain; red arrows, perturbation of the gizzard mesoderm. (B) Serial longitudinal sections of E9 RCAS-*Scleraxis* and RCAS-GFP stomachs analyzed by in situ hybridization with specific *Scleraxis* and *Type I Collagen* riboprobes, and by immunohistochemistry with anti-GAG (3C2) and anti- α SMA antibodies. Areas with many RCAS-*Scleraxis*-expressing cells, detected by the anti-GAG antibody, are associated with inhibition of α SMA expression, but not with an induction of *Type I Collagen* expression. Black arrows indicate endogenous tendon structures; red arrows, ectopic *Scleraxis* expression domains. (C) Serial longitudinal sections of E9 stomach infected with RCAS-*Scleraxis*-*Engrailed* or RCAS-GFP retroviruses analyzed by in situ hybridization with *Env* and *Type I Collagen* riboprobes, and by immunohistochemistry with anti- α SMA and 3C2 antibodies. The misexpression of *Scleraxis*-*Engrailed* in tendon domains is associated with the repression of *Type I Collagen* expression in the infected tendon and defective tendon structures. Misexpression of GFP had no effect on tendon development. Black arrows indicate endogenous tendon structures; red arrows, *Scleraxis*-*Engrailed* expression domains. (D) *Scleraxis* misexpression in the gizzard increases *Tenomodulin* expression. Quantitative-RT-PCR experiments on E9 stomachs in which RCAS-GFP (control), RCAS-*Scleraxis* or RCAS-*Scleraxis*-*Engrailed* were misexpressed. RCAS-*Scleraxis* infected gizzards express 4.2-fold more *Tenomodulin* than do controls, whereas RCAS-*Scleraxis*-*Engrailed* infected gizzards express 90% less *Tenomodulin* transcripts than do controls. Ectopic expression of *Scleraxis* in the proventriculus does not induce *Tenomodulin* in this tissue. Each measurement was done on three independent cDNA preparations ($n=4$).

These data suggest that E5 gizzard undifferentiated mesenchyme can differentiate into at least two distinct cell types: visceral SMC and tendon cells. These data also indicate that the FGF pathway and *Scleraxis* are essential for the formation and differentiation of intermuscular tendons.

DISCUSSION

In this work, we show that embryonic stomach is characterized by the presence of two tendon domains (intermuscular tendons) close to the gastric visceral smooth muscle structures. Moreover, we propose that coordinated development of the tendon and gastric

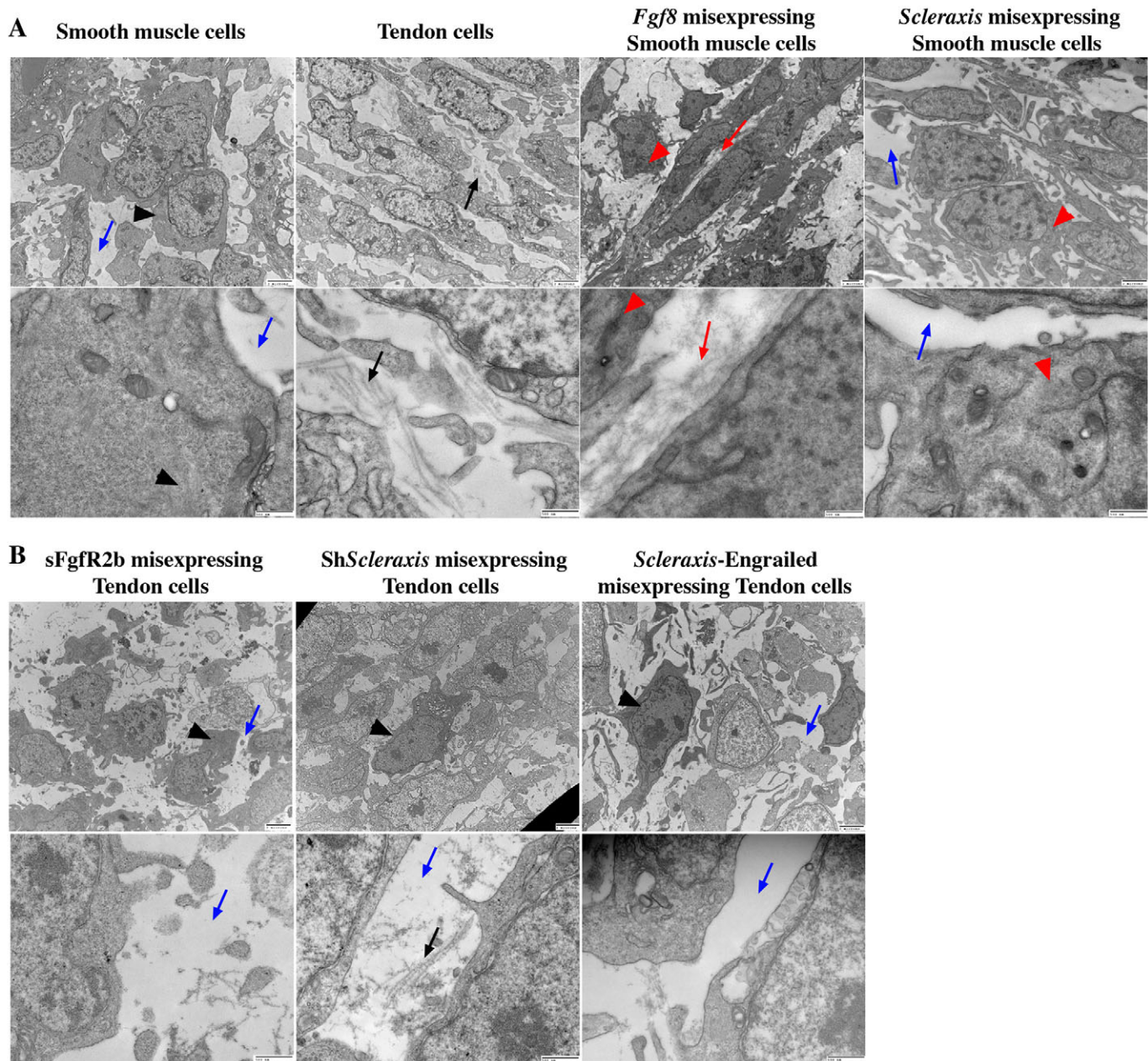


Fig. 5. Ultrastructural analysis of E9 gizzard sections following retroviral misexpression. (A) Analysis of E9 gizzard misexpressing GFP, *Fgf8* or *Scleraxis*. Control (RCAS-GFP) SMCs are rounder with few mitochondria and have actin filaments in the cytoplasm. Control tendon cells are aligned and surrounded by collagen fibrils. In addition, they show predominantly rough endoplasmic reticulum and mitochondria. RCAS-*Fgf8* SMCs present aberrant filopodia, no intracellular actin formation and numerous organelles. RCAS-*Scleraxis* SMC also show aberrant filopodia, disorganized intracellular actin and an increased number of organelles. *Fgf8* misexpression is also associated with ectopic collagen fibrils in the intercellular region that are not observed in RCAS-*Scleraxis* SMC. Black arrows indicate extracellular collagen fibrils; black arrowheads, intracellular actin formation; blue arrows, the absence of extracellular matrix; red arrows, ectopic collagen fibrils; red arrowheads, the absence of intracellular actin formation. (B) Analysis of tendon cells from E9 gizzards misexpressing *sFgfR2b*, *ShScleraxis* or *Scleraxis-Engrailed*. RCAS-*sFgfR2b* tendon cells present aberrant morphology with dark cytoplasm (arrowhead), and without collagen fibrils (blue arrows). RCAS-*ShScleraxis* tendon cells present a moderate phenotype with a strong decrease of collagen fibril production (blue and black arrows), dark cytoplasm and rounder morphology (arrowhead). RCAS-*Scleraxis-Engrailed* gizzards also have tendon cells with dark cytoplasm (arrowhead) and a strong inhibition of collagen fibril production (blue arrow). Scale bars: 2 μ m (upper panels) and 500 nm (lower panels).

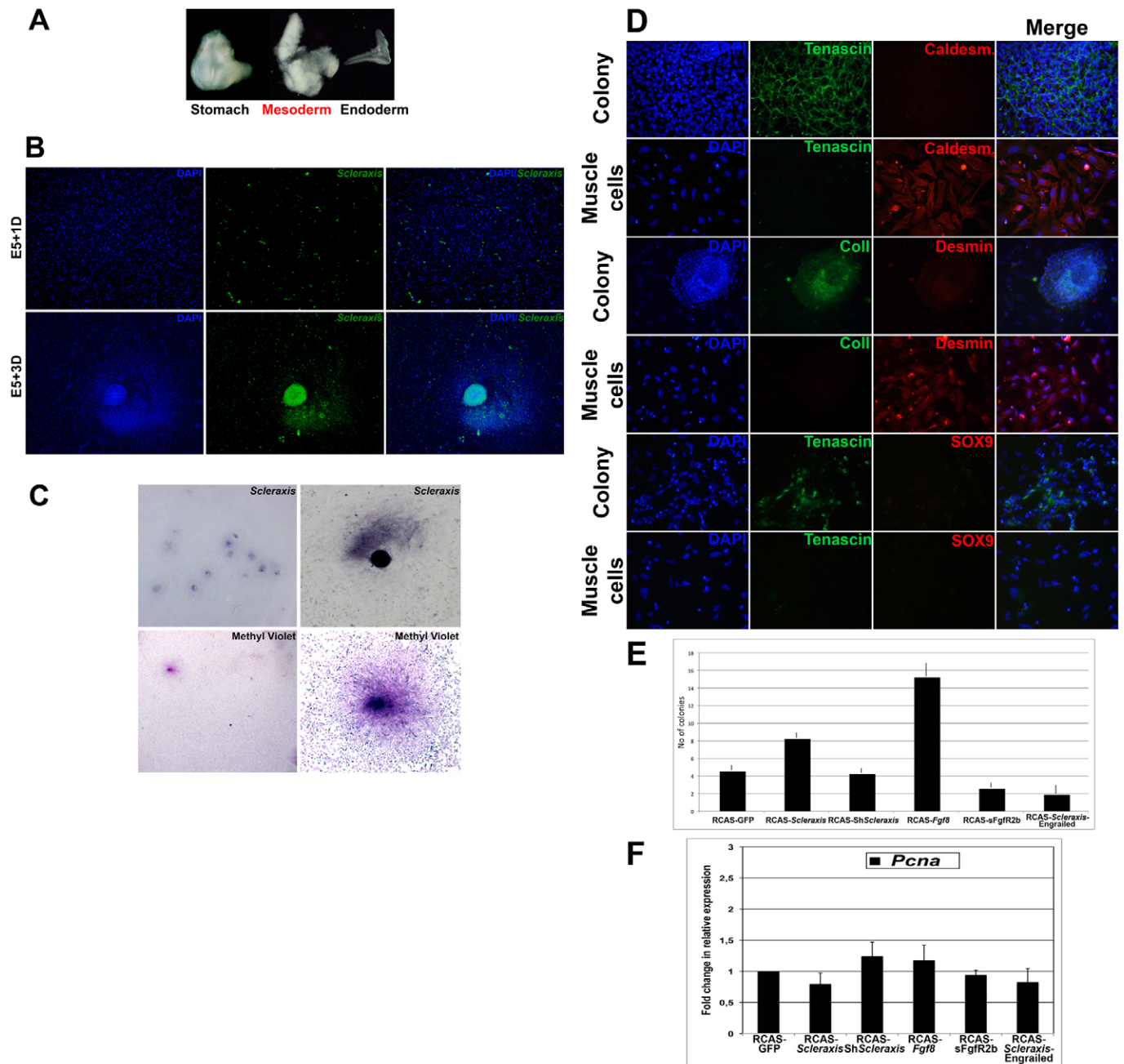


Fig. 6. Characterization of distinct cell populations in primary cell cultures derived from E5 gizzard mesenchyme. (A) Enzymatic dissociation and microdissection of an E5 gizzard into mesenchyme and endoderm. The undifferentiated mesenchymal cells will be cultured for one (E5+1D) and three days (E5+3D). (B) In cellulo in situ hybridization using the antisense *Scleraxis* riboprobe on E5+1D and E5+3D mesenchymal-derived cells. Nuclei were visualized with DAPI. At E5+1D, *Scleraxis*-positive cells are isolated (upper panel), whereas at E5+3D they have aggregated into colonies (lower panel). *Scleraxis* expression is colored using the Photoshop software. (C) Analysis of E5+3D mesenchymal-derived cells by in cellulo in situ hybridization using the antisense *Scleraxis* riboprobe (upper panel) and Methyl Violet staining (lower panel). Clusters of cells expressing *Scleraxis* are also positive for Methyl Violet, a dye that labels cells containing high-level organelles. (D) Characterization of E5+3D mesenchymal-derived cells by immunofluorescence. Nuclei were visualized with DAPI. The tendon-specific markers Tenascin and Type I Collagen were used, as well as the SMC marker Caldesmon, the mesenchymal cell marker Desmin, and the chondrocyte marker Sox9. Colonies were all positive for the tendons markers, but not for Caldesmon or Sox9. The scattered cells adjacent to the colonies presented strong expression of muscle markers, but no expression of tendon or chondrocyte markers. These results demonstrate that the mesenchymal-derived cultures contain two types of cells: tendon cells aggregated into colonies, and SMC, represented by the scattered cells. (E) Colony-forming efficiency assessed by Methyl Violet staining of E5+3D primary cells derived from the mesenchyme of gizzards and infected with RCAS-GFP, RCAS-*Scleraxis*, RCAS-Sh*Scleraxis*, RCAS-*Fgf8*, RCAS-sFgfR2b or RCAS-*Scleraxis*-Engrailed for three days. *Fgf8* and *Scleraxis* misexpression have a strong positive effect on the number of colonies, while Sh*Scleraxis* misexpression moderately inhibits their formation. *Scleraxis*-Engrailed and sFgfR2 are both potent inhibitors of cell cluster formation. Each measurement was done on three independent experiments ($n=3$). (F) Analysis of *Pcna* expression by quantitative RT-PCR amplification of E5+3D culture cells following infection with different retroviral constructs. Each measurement was done on two independent cDNA preparations ($n=4$). Perturbation of *Scleraxis* expression by different means has a moderate impact on *Pcna* expression.

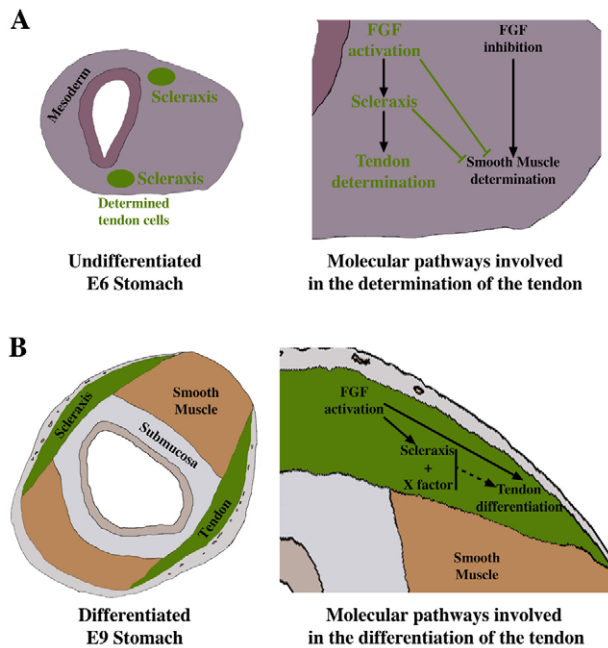


Fig. 7. Model of the molecular pathways and the tissue interactions during stomach development. (A) Schematic representations of avian E6 stomach and the molecular pathways involved in the determination of the tendon domains. At E6, the mesenchymal layer is composed of undifferentiated visceral mesenchyme and two emerging committed tendon cell domains (green areas). The cells of these domains, upon mesenchymal FGF activation, express *Scleraxis* and become committed to the tendon lineage, while their differentiation into SMC is inhibited. (B) Schematic representations of avian E9 stomach and the molecular pathways involved in the differentiation of the intermuscular tendons. At E9, the mesenchymal layer is divided in two differentiated visceral SMC domains (brown areas), submucosa (gray area) and two well-organized tendon domains (green areas). Mesenchymal FGF activation allows the differentiation of the tendons that express *Scleraxis*. *Scleraxis* with additional transcription factors or interacting partners (X factor) might ensure the differentiation of tendon cells.

smooth muscle structures is necessary to ensure the correct development of the stomach. This notion is supported by the findings that: (1) the inhibition of tendon formation induced stomach malformations; and (2) the increase of tendon territories happened at the expense of those of visceral SMCs and impaired their differentiation *in vivo*. Moreover, we show that undifferentiated stomach mesenchyme can give rise to both SMC and tendon cells, suggesting that the development of the intermuscular tendon cells progresses an autonomous way from the stomach mesenchyme, through the FGF pathway and under *Scleraxis* control.

Presence of intermuscular tendons in the stomach

The majority of smooth muscle forms continuous structures devoid of attachments. However, a few smooth muscles are attached to rigid structures (i.e. the anococcygeus, the rectococcygeus and the costouterus muscles) (Gabella, 1985). The rectococcygeus muscle, for instance, is attached to the anterior surface of the second and third coccygeal vertebrae, and is inserted onto the posterior surface of the rectum through anchoring tendons. In this study, we describe two tendons that connect two smooth muscle bundles in the stomach. The

connection of two muscle bundles through a connective structure, which is defined as an intermuscular tendon, has been previously described; for example, in the diaphragm (Ackerman and Greer, 2007). The localization of two intermuscular tendons in the stomach suggests that their physiological role is to diminish the high tension generated by the periodic contraction of the powerful stomach smooth muscle structures.

In this study, we found that some specific tendon markers (i.e. *Scleraxis*, *Tenomodulin*, *Four jointed*, *Type I Collagen* and *Decorin*) are associated with the development and differentiation of these structures. However, other limb tendon-specific markers are not expressed. Indeed, a putative target gene of *Scleraxis*, *Type XIV Collagen* is not expressed in the intermuscular tendons but is expressed in the gastric ENS cells. These molecular differences between intermuscular tendons and force-transmitting or anchoring tendons suggest that the generation of tendon structure or the organization of the tissue attachment in these tendon subgroups requires molecular modulation.

Determination of the intermuscular tendon domain

At E6, *Scleraxis* expression defines two domains that give rise to the tendon structures of the stomach (Fig. 7). These two domains are induced by the mesenchymal FGF signaling pathway. We also demonstrate that inactivation of *Scleraxis* expression extinguishes the tendon domains, whereas ectopic expression blocks the differentiation of the visceral mesenchyme into SMC. Tendons are defined as the connective tissues that connect/attach muscle to bone (musculoskeletal system) and muscle to muscle (diaphragm system) (Tozer and Duprez, 2005; Ackerman and Greer, 2007). Tendon cells can have different embryological origins; for instance, body wall tendons derive from one specific somitic compartment, the syndetome (Brent et al., 2003), and craniofacial tendons from cranial neural crest cells (Crane and Trainor, 2006). No embryonic origin was demonstrated for the intermuscular tendons in the diaphragm (Ackerman and Greer, 2007). The digestive tract mesenchyme derives from the splanchnopleural mesoderm and is also colonized by neural crest-derived (Le Douarin and Teillet, 1973; Barlow et al., 2008) and mesothelium-derived vascular SMC (Wilm et al., 2005) cells. Chick/quail chimera experiments demonstrated that colonization by neural crest-derived cells of the stomach gives rise to ENS cells (Le Douarin and Teillet, 1973) and not to the tendon domains we identified in this work. An early study of the muscle-tendon structures in the avian gizzard noted the intimate relationship between muscle bundles and tendons in this organ, and suggested that both derive from the same cell type (Watzka, 1932). Our finding that mesenchymal FGF signaling triggers *Scleraxis* expression and, consequently, the determination of the two tendon domains *in vivo* and in primary cell culture suggests that, upon FGF activation, selected stomach mesenchymal cells are primed to differentiate into tendon cells and to express *Scleraxis*.

Differentiation of the intermuscular tendon structure

As previously reported (Brent and Tabin, 2004; Edom-Vovard et al., 2002), we found that the mesenchymal FGF signaling pathway positively regulates *Scleraxis* expression and induces differentiation of the two tendon structures and the expression of differentiation markers, such as *Type I Collagen* and *Tenomodulin*, in different parts of the digestive tract. Conversely, *Scleraxis* is essential for the development of the tendons and *Tenomodulin* expression. However,

Scleraxis misexpression alone cannot induce ectopic expression of *Type I Collagen*, whereas the transcriptional repressor *Scleraxis-Engrailed* inhibits *Type I Collagen* expression in vivo. *Scleraxis* is a bHLH transcription factor that can interact with the bHLH factor E47 to regulate the expression of *Type I Collagen* in tendon fibroblasts (Lejard et al., 2007). All these data suggest that *Scleraxis* requires additive transcription factors or interacting partners to control the differentiation process initiated by activation of the FGF pathway. We can also imagine that *Scleraxis* proteins present in the musculoskeletal or in the intermuscular tendons might interact with different tissue-specific partner(s) to reinforce these tissue specificities. In addition, other signaling pathways activated by FGF can cooperate with *Scleraxis* to induce tendon differentiation. Different studies showed that the FGF-WNT regulatory network controls mesenchyme development. Recently, mesenchymal FGF signaling has been reported to regulate β -catenin-mediated WNT signaling in lung mesenchyme (Yin et al., 2008). The canonical Frizzled receptor *Fz8* is expressed in the stomach (Theodosiou and Tabin, 2003) and its expression pattern overlaps with that of *Scleraxis*, which suggests that *Scleraxis* and the WNT canonical pathways are induced after activation of the FGF pathway. In future studies we will try to identify the WNT ligand that interacts with *Fz8* and that might enable the cooperation with *Scleraxis*.

In summary, we show that the vertebrate stomach harbors two tendon domains located in the antrum/muscular stomach, which are closely associated with the visceral smooth muscle structures. The possible physiological function of these domains might be to ensure elasticity of the stomach during contraction of the two massive visceral muscles.

We thank Drs D. Duprez, P. Francis-West, A. Neubuser and C. Tabin for reagents. We thank Dr S. Faure and the members of INSERM ERI 25 for discussions. This work was supported by grants from INSERM, Agence Nationale pour la Recherche (ANR-07-JCJC-0112), Association Française contre les Myopathies (Number 11877) and Association contre le Cancer (Number 3725) to P.d.S.B. L.I.G. was supported by the Ministère de l'Éducation et de la Recherche, and C.N. by an AFM postdoctoral fellowship.

Supplementary material

Supplementary material for this article is available at <http://dev.biologists.org/cgi/content/full/136/5/791/DC1>

References

- Ackerman, K. G. and Greer, J. J. (2007). Development of the diaphragm and genetic mouse models of diaphragmatic defects. *Am. J. Med. Genet. C Semin. Med. Genet.* **145C**, 109-116.
- Barlow, A. J., Wallace, A. S., Thapar, N. and Burns, A. J. (2008). Critical numbers of neural crest cells are required in the pathways from the neural tube to the foregut to ensure complete enteric nervous system formation. *Development* **135**, 1681-1691.
- Bi, Y., Ehrichtou, D., Kilts, T. M., Inkson, C. A., Embree, M. C., Sonoyama, W., Li, L., Leet, A. I., Seo, B. M., Zhang, L. et al. (2007). Identification of tendon stem/progenitor cells and the role of the extracellular matrix in their niche. *Nat. Med.* **13**, 1219-1227.
- Brent, A. E. and Tabin, C. J. (2004). FGF acts directly on the somitic tendon progenitors through the Ets transcription factors *Pea3* and *Erm* to regulate *scleraxis* expression. *Development* **131**, 3885-3896.
- Brent, A. E., Schweitzer, R. and Tabin, C. J. (2003). A somitic compartment of tendon progenitors. *Cell* **113**, 235-248.
- Crane, J. F. and Trainor, P. A. (2006). Neural crest stem and progenitor cells. *Annu. Rev. Cell Dev. Biol.* **22**, 267-286.
- de Santa Barbara, P., van den Brink, G. R. and Roberts, D. J. (2002). Molecular etiology of gut malformations and diseases. *Am. J. Med. Genet.* **115**, 221-230.
- de Santa Barbara, P., Williams, J., Goldstein, A. M., Doyle, A. M., Nielsen, C., Winfield, S., Faure, S. and Roberts, D. J. (2005). Bone morphogenetic protein signaling pathway plays multiple roles during gastrointestinal tract development. *Dev. Dyn.* **234**, 312-322.
- Edom-Vovard, F., Bonnin, M. and Duprez, D. (2001). *Fgf8* transcripts are located in tendons during embryonic chick limb development. *Mech. Dev.* **108**, 203-206.
- Edom-Vovard, F., Schuler, B., Bonnin, M. A., Teillet, M. A. and Duprez, D. (2002). *Fgf4* positively regulates *scleraxis* and *tenascin* expression in chick limb tendons. *Dev. Biol.* **247**, 351-366.
- Gabella, G. (1985). Chicken gizzard. The muscle, the tendon and their attachment. *Anat. Embryol.* **171**, 151-162.
- Gabella, G. (2002). Development of visceral smooth muscle. *Results Probl. Cell Differ.* **38**, 1-37.
- Gregoire, D., Brodolin, K. and Mechali, M. (2006). *HoxB* domain induction silences DNA replication origins in the locus and specifies a single origin at its boundary. *EMBO Rep.* **7**, 812-816.
- Hamburger, V. and Hamilton, H. L. (1951). A series of normal stages in the development of the chick embryo. *J. Morphol.* **88**, 49-92.
- Harpavat, S. and Cepko, C. L. (2006). RCAS-RNAi: a loss-of-function method for the developing chick retina. *BMC Dev. Biol.* **6**, 2.
- Le Douarin, N. M. and Teillet, M. A. (1973). The migration of neural crest cells to the wall of the digestive tract in avian embryo. *J. Embryol. Exp. Morphol.* **30**, 31-48.
- Lefebvre, V., Huang, W., Harley, V. R., Goodfellow, P. N. and de Crombrughe, B. (1997). *SOX9* is a potent activator of the chondrocyte-specific enhancer of the pro $\alpha 1(I)$ collagen gene. *Mol. Cell. Biol.* **17**, 2336-2346.
- Lejard, V., Brideau, G., Blais, F., Salingcarnboriboon, R., Wagner, G., Roehrl, M. H., Noda, M., Duprez, D., Houillier, P. and Rossert, J. (2007). *Scleraxis* and *NFATc* regulate the expression of the pro- $\alpha 1(I)$ collagen gene in tendon fibroblasts. *J. Biol. Chem.* **282**, 17665-17675.
- Mandler, M. and Neubuser, A. (2004). FGF signaling is required for initiation of feather placode development. *Development* **131**, 3333-3343.
- McLelland, J. (1979). *Systema digestorium*. In *Nomina Anatomica Avium* (ed. J. J. Baumel), pp. 267-285. London: Academic Press.
- Mericiskay, M., Blanc, J., Tritsch, E., Moriez, R., Aubert, P., Neunlist, M., Feil, R. and Li, Z. (2007). Inducible mouse model of chronic intestinal pseudo-obstruction by smooth muscle-specific inactivation of the *SRF* gene. *Gastroenterology* **133**, 1960-1970.
- Moniot, B., Biau, S., Faure, S., Nielsen, C. M., Berta, P., Roberts, D. J. and de Santa Barbara, P. (2004). *SOX9* specifies the pyloric sphincter epithelium through mesenchymal-epithelial signals. *Development* **131**, 3795-3804.
- Murchison, N. D., Price, B. A., Conner, D. A., Keene, D. R., Olson, E. N., Tabin, C. J. and Schweitzer, R. (2007). Regulation of tendon differentiation by *scleraxis* distinguishes force-transmitting tendons from muscle-anchoring tendons. *Development* **134**, 2697-2708.
- Nielsen, C., Murtaugh, L. C., Chung, J. C., Lassar, A. and Roberts, D. J. (2001). Gizzard formation and the role of *Bapx1*. *Dev. Biol.* **231**, 164-174.
- Niessen, P., Rensen, S., van Deursen, J., De Man, J., De Laet, A., Vanderwinden, J. M., Wedel, T., Baker, D., Doevendans, P., Hofker, M. et al. (2005). Smoothelin-a is essential for functional intestinal smooth muscle contractility in mice. *Gastroenterology* **129**, 1592-1601.
- Roberts, D. J. (2000). Molecular mechanisms of development of the gastrointestinal tract. *Dev. Dyn.* **219**, 109-120.
- Roberts, D. J., Smith, D. M., Goff, D. J. and Tabin, C. J. (1998). Epithelial-mesenchymal signaling during the regionalization of the chick gut. *Development* **125**, 2791-2801.
- Ros, M. A., Rivero, F. B., Hinchliffe, J. R. and Hurle, J. M. (1995). Immunohistological and ultrastructural study of the developing tendons of the avian foot. *Anat. Embryol. (Berl.)* **192**, 483-496.
- Schweitzer, R., Chung, J. H., Murtaugh, L. C., Brent, A. E., Rosen, V., Olson, E. N., Lassar, A. and Tabin, C. J. (2001). Analysis of the tendon cell fate using *Scleraxis*, a specific marker for tendons and ligaments. *Development* **128**, 3855-3866.
- Shukunami, C., Takimoto, A., Oro, M. and Hiraki, Y. (2006). *Scleraxis* positively regulates the expression of *tenomodulin*, a differentiation marker of tenocytes. *Dev. Biol.* **298**, 234-247.
- Simon-Assmann, P. and Kédinger, M. (2000). Tissue recombinants to study extracellular matrix targeting to basement membranes. *Methods Mol. Biol.* **139**, 311-319.
- Theodosiou, N. A. and Tabin, C. J. (2003). Wnt signaling during development of the gastrointestinal tract. *Dev. Biol.* **259**, 258-271.
- Tozer, S. and Duprez, D. (2005). Tendon and ligament: development, repair and disease. *Birth Defects Res. C Embryo Today* **75**, 226-236.
- Wallace, A. S. and Burns, A. J. (2005). Development of the enteric nervous system, smooth muscle and interstitial cells of Cajal in the human gastrointestinal tract. *Cell Tissue Res.* **319**, 367-382.
- Watzka, M. (1932). Sehnen glatter Muskelfasern. *Z. mikr-anat Forsch* **30**, 23-28.
- Wilm, B., Ipenberg, A., Hastie, N. D., Burch, J. B. and Bader, D. M. (2005). The serosal mesothelium is a major source of SMCs of the gut vasculature. *Development* **132**, 5317-5328.
- Yamaguchi, K., Parish, J., Akita, K. and Francis-West, P. (2006). Developmental expression of the chick four-jointed homologue. *Dev. Dyn.* **235**, 3085-3091.
- Yin, Y., White, A. A., Huh, S.-U., Hilton, M. J., Kanazawa, H., Long, F. and Ornitz, D. M. (2008). An FGF-WNT gene regulatory network controls lung mesenchyme development. *Dev. Biol.* **319**, 426-436.

Table S1. Data set of selected genes identified through the microarray screen using E6 and E9 chick gizzards

Gene	E6 Gizzard			E9 Gizzard		
	Signal	Detection	Detection <i>P</i> -value	Signal	Detection	Detection <i>P</i> -value
<i>SRF</i>	267.8	P	0.000244	591.7	P	0.000244
<i>Scleraxis</i>	112.2	P	0.00293	300.7	P	0.000244
<i>Smoothelin</i>	78.1	P	0.001953	189.8	P	0.001953
<i>Caldesmon</i>	2473.5	P	0.000244	4930.7	P	0.000244
<i>Lumican</i>	795	P	0.000244	1554.5	P	0.000244
<i>Desmin</i>	46	A	0.095215	200.2	P	0.010742
<i>Smooth muscle actin, gamma 2</i>	1859.1	P	0.000244	8764.5	P	0.000244
<i>Smooth muscle myosin, heavy chain 11</i>	1121.4	P	0.000244	3508.3	P	0.000244
<i>Tenomodulin</i>	33.8	P	0.023926	629.2	P	0.000244
<i>Bmp4</i>	3.6	A	0.533936	89.3	P	0.000732
<i>Collagen, type XII, alpha 1</i>	128.9	P	0.000244	1153.7	P	0.000732
<i>Decorin</i>	2929.1	P	0.000244	4458	P	0.000244
<i>BmpRII</i>	86.4	P	0.018555	2.9	A	0.888428
<i>BmpR1B</i>	285.2	P	0.000244	133	P	0.00293
<i>Fibroblast growth factor 10</i>	200.2	P	0.005859	40.9	A	0.35791
<i>HoxA5</i>	194.9	P	0.000732	64.5	A	0.067627
<i>Myocardin</i>	142.9	P	0.008057	45.7	A	0.303711
<i>BmpR1A</i>	61.5	P	0.01416	39.8	A	0.27417
<i>Shh</i>	87.4	P	0.030273	93.3	P	0.018555
<i>Patched domain containing 1</i>	258.5	P	0.010742	276.2	P	0.01416
<i>Sox10</i>	224.1	P	0.001953	216.2	P	0.00293
<i>HoxB4</i>	75.3	P	0.018555	71.7	A	0.111572
<i>BarX-1</i>	2410	P	0.000244	2920.3	P	0.000244